Accepted Manuscript

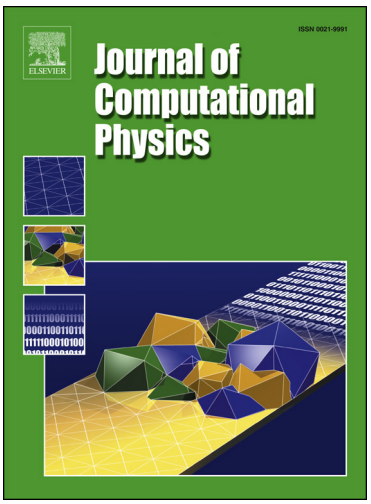

Multiresolution Operator Decomposition for Flow Simulation in Fractured Porous Media

Qingfu Zhang, Houman Owhadi, Jun Yao, Florian Schäfer, Zhaoqin Huang, Yang Li

PII: S0021-9991(19)30013-0
DOI: https://doi.org/10.1016/j.jcp.2018.12.032
Reference: YJCPH 8429

To appear in: *Journal of Computational Physics*

Received date: 8 November 2017
Revised date: 16 October 2018
Accepted date: 29 December 2018

Please cite this article in press as: Q. Zhang et al., Multiresolution Operator Decomposition for Flow Simulation in Fractured Porous Media, *J. Comput. Phys.* (2019), https://doi.org/10.1016/j.jcp.2018.12.032

Multiresolution Operator Decomposition for Flow Simulation in Fractured Porous Media

Qingfu Zhang [a,b], Houman Owhadi [b], Jun Yao [a*], Florian Schäfer [b], Zhaoqin Huang [a], Yang Li[a]

[a] China University of Petroleum (East China), Qingdao 266580, China

[b] California Institute of Technology, Pasadena, CA 91125

Abstract

Fractures should be simulated accurately given their significant effects on whole flow patterns in porous media. But such high-resolution simulation imposes severe computational challenges to numerical methods in the applications. Therefore, the demand for accurate and efficient technique is widely increasing. A near-linear complexity multiresolution decomposition is proposed for solving flow problems in fractured porous media. In this work, Discrete Fracture Model (DFM) is used to describe fractures, in which the fractures are explicitly represented as (n-1) dimensional elements. The solution space is decomposed into several subspaces and we then compute the corresponding solutions of DFM in each subspace. The pressure distribution of fractured porous media is obtained by combing the DFM solutions of all subspaces. Numerical results are presented to demonstrate the accuracy and efficiency of the proposed multigrid method. The comparisons with standard method show that the proposed multigrid method is a promising method for flow simulation in fractured porous media.

Keywords

Multigrid method; Discrete fracture model; Flow simulation; Fractured porous media; Multiresolution decomposition

1. Introduction

Subsurface flows in porous media are impacted by heterogeneities in multiscale scales. It is a challenging problem to solve numerically all the scales. Apart from the rough heterogeneous properties, these porous media commonly contain fractures, which will seriously aggravate the heterogeneity. These heterogeneous characteristics should be taken seriously given their significant influence on whole flow patterns. However, the porous flow problems with rough permeability fields impose great difficulties on the direct numerical simulation. The necessary resolution solutions may need several millions of grid cells which are computationally costly.

Among the flow models aimed at representing fractures effectively, dual-porosity model [1-2] supposes that the fractures are highly permeable and interconnected with each other. Although this model is widely applied in the field, researches show that it is only available for the porous media in which the fractures are highly developed. Furthermore, this method could not efficiently model the fluid flow in the large-scale fractures [3]. Large-scale fractures were then described explicitly with single-porosity model in which fractures are regarded as narrow region [4]. Obviously, this model has an expected resolution, but it has to suffer a complicated computation and grid generation process. Equivalent continuum model [36-38] is instead used to form an equivalent permeability field to describe the heterogeneity of the fractured porous media. While ECM is efficient and convenient, it works well only when there exists REV in the fractured media [36]. As an alternative, the discrete fracture model (DFM) is developed [5-9]. The n-D fractures are simplified to (n-1)-D elements using the flux equivalent theory. That is, taking the 2D problems for example, the fracture is treated as a line element and matched grid system is applied. That is the fractures are regarded as inner boundaries of the region. Therefore, DFM is appealing for its ability to avoid the complicated grid generation inside the fractures.

Although DFM is attractive for its simple and efficiency, it is deemed intractable for implement in application as there were no efficient numerical methods could solve DFM fast and accurately. A large amount of CPU time and compute memory are needed which may beyond the controllable level. This issue motivated the development of fast numerical methods.

During the past few years, numerical homogenization was applied as fast methods to model fluid flow in heterogeneous porous media, including upscaling techniques [10-11], multiscale methods [12-15] etc. Recently, multiscale methods have been extended to conduct flow simulation in fractured porous media [16-19] by

using multiscale functions to capture the heterogeneous information on the fine-scale. Although numerical homogenization has obtained satisfying results, and made contributions to the development of fast methods toward fractured porous media, there are difficulties in the identification of interpolation and restriction process [31]. Given multigrid methods are now well known as being one of the fastest for solving elliptic problems [20-23], in this paper, we propose a multigrid formulation for flow simulation in fractured porous media.

While multigrid methods have been effectively extended to solve many kinds of partial differential equations, their convergence rate can be severely affected by the lack of regularity of coefficients [24-25]. Therefore, their ability for flow simulation is limited by the intrinsic strong heterogenous permeability field in porous media. Even though some improved multigrid methods could achieve robustness to some extent [26-29], the design of multigrid methods that are provably robust with respect to rough coefficients was an open problem of practical importance [30] as introduced in [31-32]. Alternative methods such as [33-35] are able to obtain a multiresolution compression of the solution space, however their ability to solve PDEs is impacted by the regularity of coefficients. Hence, it is desirable to develop a method that could lower the computational complexity.

In this paper, we introduce a near-linear complexity multiresolution operator decomposition method (multigrid method) [32] and extend it to simulation of fluid flow in porous media. Then we continue the research and successfully capture the influences of fractures in fractured porous media. Gamblets are derived from a Bayesian and a game theoretic approach to numerical homogenization with a priori rigorous exponential decay estimates [39]. These constructed gamblets (1) are elementary solutions of hierarchical information games associated with the process of computing with partial information and limited resources, (2) have a natural Bayesian interpretation under the mixed strategy emerging from the game theoretic formulation, (3) this method could realize its fast simulation by decomposing the solution space into a direct sum of linear subspace that are orthogonal.

The proposed Gamblets are identified by conditioning Gaussian fields. They are represented as the optimal recovery splines and analyzed through their variational (energy minimizing) characterization. Therefore, Gamblets is a kind of energy minimization methods which can be traced back to optimal recovery splines [43-44]. Many methods can be represented as optimal recovery splines, such as Polyharmonic Splines [55-58] and Rough Polyharmonic Splines [45]. The basis functions

constructed by Variational Multiscale Method [46] and Local Orthogonal Decomposition Method (LOD) [47] can also be represented as optimal recovery splines. The energy minimizing basis functions ψ_i of [48-51] are identified by minimizing the total $\sum_i \|\psi_i\|^2$ subject to the global constraint $\sum_i \psi_i(x)=1$ can also be identified as approximate optimal recovery splines if the energy minimization is done separately for each spline subject to local (rather than global) constraints.

Gamblets are defined with minimizers of $\|\psi\|_\lambda = \int_\Omega \nabla\psi^T \lambda \nabla\psi \, dx$ subject to $\int_\Omega \phi_j \psi = \delta_{ij}$. Rough Polyharmonic Splines [45] can be recovered as a particular case of gamblets. The basis functions of the LOD method can also be recovered as a particular case of gamblets by selecting the measurement functions $\phi_i = \sum_{j=1}^m M_{i,j}^{-1}\varphi_j$, with φ_j are piecewise linear nodal basis functions and $M_{i,j}=\int_\Omega \varphi_i\varphi_j$. Although both Gamblets and the LOD method lead to an orthogonal decomposition of the solution space the two approaches differ in the following points: (a) by using measurement functions defined by elements ϕ_i of the dual space rather than through a correction of classical conforming finite elements φ_i, gamblets avoid the requirement for conforming measurement functions and the optimal L^2 projection properties of the Clément interpolation operator (used in [47] to derive exponential decay estimates). (b) The derivation of a corresponding multiresolution method is not based on a hierarchy of corrections of a hierarchy of conforming finite elements but on the pull back of a hierarchy of elements of the dual space.

Constrained energy minimization is also used to construct multiscale basis functions in multiscale finite element method (MsFEM) [53-54] to obtain a mesh-dependent convergence. Both gamblets and MsFEM produce numerical homogenization basis functions but it is not clear how to turn MsFEM into a hierarchy while preserving rigorous a priori near linear complexity versus accuracy estimates.

This paper proceeds as follows: we start by introducing the governing equations of fluid flow in fractured media, including mathematical model of discrete fracture network. Next, we introduce the multiresolution operator decomposition briefly. Then the multiresolution operator decomposition method is applied to solve the heterogenous porous media with rough permeability field and fractured porous media respectively. In the numerical experiment section, several numerical results are

presented to prove the validity and effectiveness of the multigrid method. Finally, the concluding remarks were given in the concluding section.

2. Governing Equations

In this work, the microfracture and matrix are treated as continuum porous media with equivalent heterogeneous permeability field. The large-scale fractures are represented with discrete fracture model (DFM). In DFM, flows in both matrix and fractures obey Darcy's law. Therefore, different from duel-continuum model [1-2], there are no separate functions designed to describe the interactions between matrix and fractures. The fracture-matrix interactions are also computed with Darcy's law [5-9]. In the porous flow domain Ω, the flow of incompressible fluid in porous media is assumed isothermal. The system consists of Darcy's law, mass balance equation.

$$-\nabla \cdot \boldsymbol{v} = q \tag{1}$$

$$\boldsymbol{v} = -\frac{\boldsymbol{K}}{\mu}\nabla p \tag{2}$$

In the above equation system, $\boldsymbol{v}$ denotes the fluid velocity; q is source/sink term; μ stands for viscosity of fluid; $\boldsymbol{K}$ denotes the permeability field; p denotes fluid pressure; we ignore the influence of gravity. Let $\boldsymbol{\lambda} = -\boldsymbol{K}/\mu$ be the mobility of fluid, and then the governing equation can be written as

$$-\nabla \cdot (\boldsymbol{\lambda}\nabla p) = q \tag{3}$$

The variational formulation of the governing equation is

$$-\iint_{\Omega} \phi \, \nabla \cdot \boldsymbol{\lambda} \, \nabla p \, \mathrm{d}\Omega = \iint_{\Omega} \phi \, q \, \mathrm{d}\Omega \tag{4}$$

For $\forall \phi \in H_0^{1,div}$. By using divergence theory, we can get

$$\iint_{\Omega} \nabla \phi \, \boldsymbol{\lambda} \, \nabla p \, \mathrm{d}\Omega = \iint_{\Omega} \phi \, q \, \mathrm{d}\Omega \tag{5}$$

In each element, p can be approximated as

$$p \approx \sum_{i=1}^{m} N_i p_i = \boldsymbol{N}(\boldsymbol{x})\boldsymbol{p} \tag{6}$$

Here m denotes the number of element nodes; $\boldsymbol{N}=[N_1, \cdots, N_m]$ is the basis function; $\boldsymbol{p}=[p_1, \cdots, p_m]$ is the pressure of fluid at the nodes.

Natural porous media exists with a heterogeneous permeability field in most cases. It is a challenging problem to develop a robust and efficient approach to solve the governing equation with rough permeability. Apart from the rough heterogeneous properties, these porous media commonly contain fractures. Fractures are formed due to the diagenesis or deformation of rock. They widely exist in naturally porous media and their presence will seriously aggravate the heterogeneity. In this work, discrete fracture model is used to represent the fractures where Darcy's law is used to model fluid flow in fractures and matrix [8]. In DFN model, the variables are assumed to be constant along the width of fracture, that is, the n-D fracture element is simplified to (n-1)-D element as shown in Fig. 1.

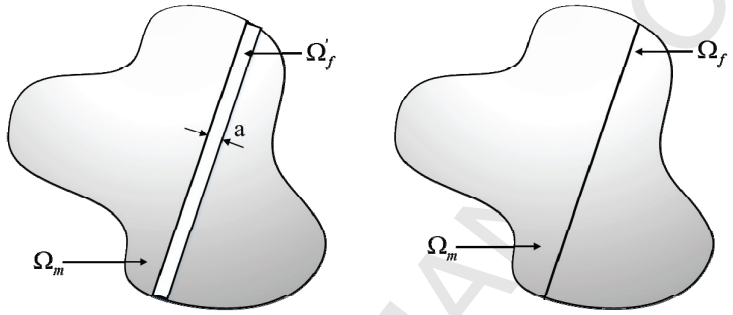

Fig.1 Schematic of discrete fracture model

Therefore, we need to discrete the governing equation in matrix system and fracture system separately. For 2D problem, 1D line segment is used to represent 2D fracture element. Then the whole domain was

$$\Omega = \Omega_m + \sum_i d_i \times \Omega_{f,i} \tag{7}$$

Here the subscript *m* and *f* denotes matrix and fracture respectively; d_i is the aperture of the *i*th fracture. Now assume the governing equation is written as *FEQ,* then the integral form in the whole domain is

$$\int_\Omega FEQ \, \mathrm{d}\Omega = \int_{\Omega_m} FEQ \, \mathrm{d}\,\Omega_m + \sum_i d_i \times \int_{\Omega_f} FEQ \, \mathrm{d}\,\Omega_{f,i} \tag{8}$$

Then the global stiffness matrix is assembled based on the superposition principle, as shown in Fig 2.

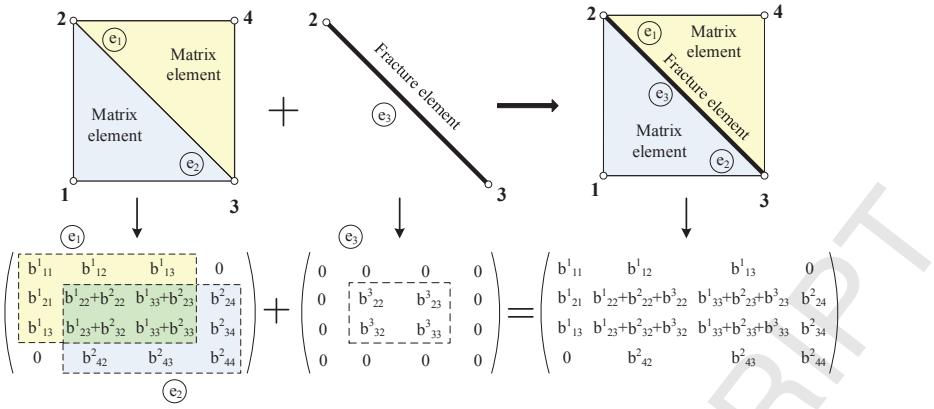

Fig.2 Schematic of stiffness matrix

That is, we treat fracture as a (n-1)-dimension element. The stiffness matrix of fracture and matrix are assembled together

$$A^f = \sum_{e=1}^{E}\left(\iint_{\Omega_{e,m}} \nabla N_{e,m}^T \, \boldsymbol{\lambda}_m \, \nabla N_{e,m} \, \mathrm{d}\Omega_{e,m} + a_f \iint_{\Omega_{e,m}} \nabla N_{e,f}^T \, \boldsymbol{\lambda}_f \, \nabla N_{e,f} \, \mathrm{d}\Omega_{e,f}\right) \quad (9)$$

Here E is the total numerical of elements, a_f is aperture of fracture, $N_{e,m}$ is basis function of matrix and $N_{e,f}$ is basis function of fracture.

Apparently traditional upscaling method must be used with great care since the fine-scale information has essential influence on whole flow patterns. This creates a motivation for the gamblets. The complexity of the method is $\mathrm{O}\left(N \log^{3d}(N)\right)$. This is a surprising near-linear complexity which will significantly save computer memory and realize fast simulation. Note that the cost of computing gamblets can be decreased to $\mathrm{O}\left(N \log^{2d+2}(N)\right)$ using incomplete Cholesky factorization as in [42].

3. Multiresolution Decomposition

The objective of the multiresolution decomposition [32] is to solve the governing equation of fluid flow as fast as possible. This method is inspired by the suggestion that this link between numerical homogenization and Bayesian inference are not coincidences [59-60], but particular instances of mixed strategies for underlying information games, and that optimal or near-optimal methods could be obtained by identifying such games and their optimal strategies.

First step to identify these games [61] is note that computation can only be done with partial information. That is, the infinite-dimensional operator (3) can only compute with finite-dimensional features of p. However, to obtain an accurate

solution one must fill the information gap between the finite-dimensional features p_m and p. that is, one should construct an interpolation operator giving p as a function of p_m. Therefore, the identification of the interpolation operator is reformulated as a minmax game where Player A chooses the source/sink term q in an admissible set, Player B is shown p_m and must give the approximation of p from the incomplete measurements. The p^* is Player A's bet, Player A's target is make the error $\|p - p^*\|_\lambda$ as big as possible and Player B's target is minimize it. A remarkable result from game theory [40-41] is that optimal strategy is mixed strategy.

To compute rapidly, the game must not be limited to filling the information gap between p_m and p. This game must be played over hierarchies of levels of complexity (e.g., one must fill information gaps between $\mathbb{R}^4$ and $\mathbb{R}^{16}$, then $\mathbb{R}^{16}$ and $\mathbb{R}^{64}$, etc). The following hierarchy of labels is introduced.

We define $\mathcal{I}^{(q)}$ is the index tree of q if it is the finite set of q-tuples of the form $i=(i_1,\ldots i_q)$. For $1 \leqslant k \leqslant q$ and $i=\left(i_1,...,i_q\right)\in \mathcal{I}^{(q)}$, let $i^{(k)}=(i_1,...,i_k)$ and $\mathcal{I}^{(k)}=\left\{i^{(k)}: i\in \mathcal{I}^{(q)}\right\}$. For $k^{'}\in\{k,...,q\}$ and $j\in \mathcal{I}^{(k^{'})}$, $j^{(k)}$ is defined as $j^{(k)}=(j_1,...,j_k)$. For $i\in \mathcal{I}^{(k)}$ and $k^{'}\in\{k,...,q\}$, we write $i^{(k,k^{'})}$ the set of elements $j\in \mathcal{I}^{(k^{'})}$ such that $j^{(k)}=i$. For $k\in\{1,...,q-1\}$, $\pi^{(k,k+1)}$ is constructed as a $\mathcal{I}^{(k)}\times\mathcal{I}^{(k+1)}$ matrix satisfying $\pi_{i,j}^{(k,k+1)}=0$ if $j\notin i^{(k,k+1)}$ and $\pi^{(k,k+1)}\left(\pi^{(k,k+1)}\right)^{\mathrm{T}}=I^{(k)}$, where $I^{(k)}$ is $\mathcal{I}^{(k)}\times\mathcal{I}^{(k)}$ identity matrix.

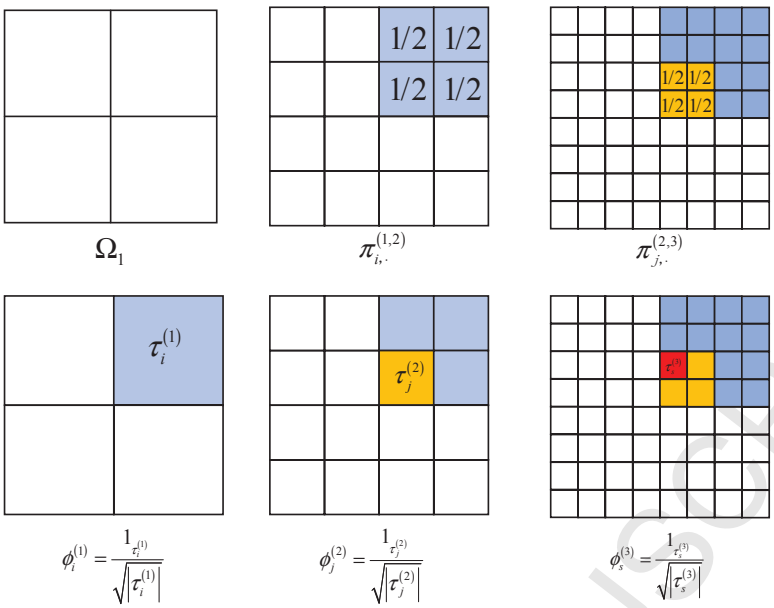

Fig.3 Schematic of grid partition of Ω

The measurement functions are defined through induction by

$$\phi_i^{(k)} = \sum_{j \in \mathcal{I}^{(k+1)}} \pi_j^{(k,k+1)} \phi_j^{(k+1)} \tag{10}$$

As shown in Fig. 3, the Ω is divided into several $2^{-k} \times 2^{-k}$ subspaces $\left(\tau_i^{(k)}\right)_{i \in \mathcal{I}^{(k)}}$. Let $\phi_i^{(k)} = 1_{\tau_i^{(k)}} / \sqrt{|\tau_i^{(k)}|}$ where $|\tau_i^{(k)}|$ is the volume of $\tau_i^{(k)}$, $1_{\tau_i^{(k)}}$ is the indicator function of $\tau_i^{(k)}$. As introduced above, we identify the gamblets by assuming that player A and player B are playing hierarchies of games. Player A chooses the source/sink term q and player B does not know his choice. Player B is shown $\left(\int_\Omega p\phi_i^{(k)}\right)_{i \in \mathcal{I}^{(k)}}$ and then gives the approximation of p and $\left(\int_\Omega p\phi_i^{(k+1)}\right)_{i \in \mathcal{I}^{(k+1)}}$ from these measurements. Player B will have a loss after he makes the choice, sees $\left(\int_\Omega p\phi_i^{(k+1)}\right)_{i \in \mathcal{I}^{(k+1)}}$ and give the approximation of p and $\left(\int_\Omega p\phi_i^{(k+2)}\right)_{i \in \mathcal{I}^{(k+2)}}$. Player A wants to make the loss of player B as big as possible to win the game, while player B tries to minimize it. The best strategy from game theory [40-41] is mixed strategy, that is player A play at random and player B replaces q with ξ in Eq. (3) to form a stochastic partial differential equation system. Player B's bet at step k is the expectation of the solution of the stochastic partial differential equation system conditioned on measurements of the solution of Eq. (1)

$$p^{(k)}(x)=\mathbb{E}\Big[v(x)\,|\,\int_\Omega v(y)\phi_i^{(k)}(y)\,\mathrm{d}y=\int_\Omega p(y)\phi_i^{(k)}(y)\,\mathrm{d}y,\ i\in I^{(k)}\Big] \tag{11}$$

Here v is the solution of the stochastic partial differential equation. The optimal strategy [32] of player B is to choose the ξ with a centered Gaussian field with covariance function $\mathcal{L}=-\mathrm{div}(a\nabla)$. In this case $p^{(k)}$ could be expressed as

$$p^{(k)}(x)=\sum_{i\in I^{(k)}}\psi_i^{(k)}(x)\int_\Omega p(y)\phi_i^{(k)}(y)\,\mathrm{d}y \tag{12}$$

The basis functions $\psi_i^{(k)}$ are referred to gamblets which represent the best bet of player B on the value of solution of the governing equation, that is

$$\psi_i^{(k)}=\mathbb{E}\Big[v\,|\,\int_\Omega v(y)\phi_j^{(k)}(y)\,\mathrm{d}y=\delta_{i,j},\ i\in I^{(k)}\Big] \tag{13}$$

However in practical computation, we will work with variational properties inherited from the conditioning of the Gaussian field v. For $i\in\{1,\ldots m\}$ consider the quadratic optimization problem

$$\begin{cases}\text{Minimize} & \|\psi\|_\lambda\\ \text{subject to} & \psi\in H_0^1(\Omega)\ \text{and}\ \int_\Omega\phi_j\psi=\delta_{ij}\ \ \text{for}\ \ j=1,\ldots,m\end{cases} \tag{14}$$

Here the $\|\psi\|_\lambda$ is the energy norm defined as $\|\psi\|_\lambda=\int_\Omega\nabla\psi^T\lambda\nabla\psi\,\mathrm{d}x$.

The following theorem shows that Eq. (14) can be used to identify ψ_i and that gamblets are characterized by optimal recovery properties.

THEOREM. It holds true that (1) the optimization problem Eq. (14) admits a unique minimizer ψ_i defined by Eq. (13), (2) for $w\in\mathbb{R}^m$, $\sum_{i=1}^m w_i\psi_i$ is the unique minimizer of $\|\psi\|_\lambda$ subject to $\int_\Omega\psi(x)\phi_j(x)=w_j$ for $j\in\{1,\ldots m\}$, and (3) $\langle\psi_i,\psi_j\rangle_\lambda=\Theta_{i,j}^{-1}$, here $\langle v,w\rangle_\lambda=\int_\Omega(\nabla v)^T\lambda\nabla w$, $\Theta_{i,j}=\int_{\Omega^2}\phi_i(x)G(x,y)\phi_j(y)\,\mathrm{d}x\mathrm{d}y$ and $G(x,y)$ is the covariance function [62] (where G is the Green's function of the governing equation).

Proof. Let $w\in\mathbb{R}^m$ and $\psi_w=\sum_{i=1}^m w_i\psi_i$ with $\psi_i=\sum_{j=1}^m\Theta_{i,j}^{-1}\int_\Omega G(x,y)\phi_j(y)\,\mathrm{d}y$.

The definition of Θ indicates that $\int_\Omega\psi_w(x)\phi_j(x)=w_j$ for $j\in\{1,\ldots m\}$. In addition,

by integration by part we get for all $\varphi \in H_0^1(\Omega)$, $\langle \psi_m, \varphi \rangle_\lambda = \sum_{i,j=1}^{m} w_i \Theta_{i,j}^{-1} \int_\Omega \phi_j \varphi$. Hence, if $\psi \in H_0^1(\Omega)$ is such that $\int_\Omega \psi(x)\phi_j(x) = w_j$ for $j \in \{1,...m\}$, then $\langle \psi_w, \psi - \psi_w \rangle_\lambda = 0$ and $\|\psi\|_\lambda^2 = \|\psi_w\|_\lambda^2 + \|\psi - \psi_w\|_\lambda^2$.

Then finish the proof of the optimality of ψ_i and ψ_w.

To make it intuitive, the illustrated $\psi_i^{(k)}$ in flow problems of porous media are shown in Fig. 4. For understandability, we consider a homogeneous porous media in this example. We suppose the incompressible fluid flows from upper boundary to bottom boundary and the left and right boundaries are treated as no-flow boundaries. Define porous flow domain $\Omega=(0,1)^2$ and let q=6.

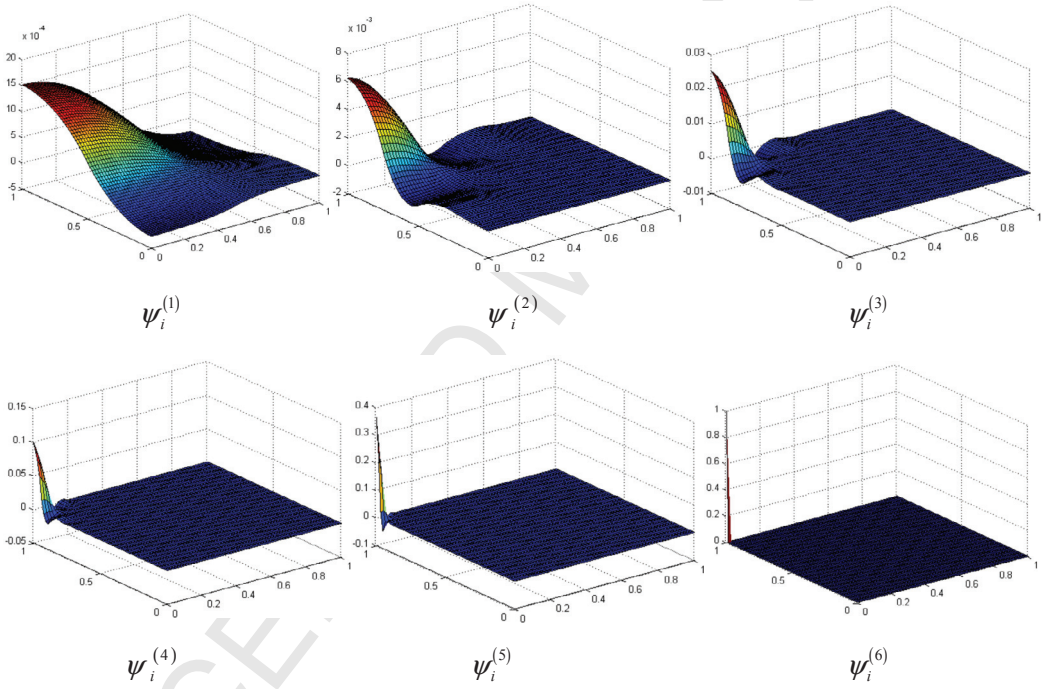

Fig.4 Illustration of $\psi_i^{(k)}$

For $k \in \{1,....,q\}$ we define the spaces

$$\mathcal{I}^{(k)} = \text{span}\left\{\psi_i^{(k)} \mid i \in \mathcal{I}^{(k)}\right\} \tag{15}$$

We can derive from Eq. (10) that the spaces are nested. Therefore, for $k \in \{1,....,q-1\}$ there is a restriction matrix $R_{i,j}^{(k,k+1)}$ such that

$$\psi_i^{(k)} = \sum_{j \in \mathcal{I}^{(k+1)}} R_{i,j}^{(k,k+1)} \psi_j^{(k+1)} \tag{16}$$

Where $R_{i,j}^{(k,k+1)}$ is a $\mathcal{I}^{(k)}\times\mathcal{I}^{(k+1)}$ matrix with the following entry

$$R_{i,j}^{(k,k+1)}=\int_\Omega \psi_i^{(k)}\phi_j^{(k+1)}=\mathbb{E}\left[\int_\Omega v(y)\phi_j^{(k+1)}(y)\,|\,\int_\Omega v(y)\phi_l^{(k)}(y)\,\mathrm{d}y=\delta_{i,l},\ l\in\mathcal{I}^{(k)}\right] \tag{17}$$

We write $A_{i,j}^{(k)}$ as the stiffness matrix of $\psi_i^{(k)}$, that is

$$A_{i,j}^{(k)}=\int_\Omega\left(\nabla\psi_i^{(k)}\right)^T\lambda\,\nabla\psi_i^{(k)} \tag{18}$$

Then the nested computation of stiffness matrix is obtained as

$$A^{(k)}=R^{(k,k+1)}A^{(k+1)}R^{(k+1,k)} \tag{19}$$

By this step, the nested computation enables one to model fluid flow in heterogeneous porous media with multigrid method. But we take a further step and introduce a multiresolution decomposition method.

For $k\in\{2,...,q\}$ let $\mathcal{J}^{(k)}$ be a k-tuples in the form $j=(j_1,...,j_k)$ and $\left\{j^{(k-1)}\,|\,j\in\mathcal{J}^{(k)}\right\}=\mathcal{I}^{(k\text{-}1)}$. Let $W^{(k)}$ be a $\mathcal{J}^{(k)}\times\mathcal{I}^{(k)}$ matrix such that for $(j,i)\in\mathcal{J}^{(k)}\times\mathcal{I}^{(k)}$ $W_{j,i}^{(k)}=0$ with $j^{(k-1)}\neq i^{(k-1)}$ and for $s\in\mathcal{I}^{(k-1)}$, $t\in\{1,...,m_s-1\}$ and $t'\in\{1,...,m_s\}$, $W_{(s,t),(s,t')}^{(k)}=\delta_{t,t'}-\delta_{t+1,t'}$. For $i\in\mathcal{J}^{(k)}$ let

$$\chi_i^{(k)}=\sum_{j=\mathcal{I}^{(k)}}W_{i,j}^{(k)}\psi_j^{(k)} \tag{20}$$

and

$$\mathcal{W}^{(k)}=\mathrm{span}\left\{\chi_i^{(k)}\,|\,i\in\mathcal{I}^{(k)}\right\} \tag{21}$$

Here $\mathcal{W}^{(k)}$ is the orthogonal complement of $\mathcal{V}^{(k\text{-}1)}$ within $\mathcal{V}^{(k)}$. Let $\oplus_\lambda$ denotes the orthogonal direct sum with respect to scalar product $\langle v,w\rangle_\lambda=\int_\Omega(\nabla v)^T\lambda\nabla w$. Then we can get the multiresolution decomposition of the space

$$\mathcal{V}^{(k)}=\mathcal{V}^{(1)}\oplus_\lambda\mathcal{W}^{(2)}\oplus_\lambda\cdots\oplus_\lambda\mathcal{W}^{(k)} \tag{22}$$

and for $k\in\{1,...,q\}$, $p^{(k+1)}-p^{(k)}$ belongs to $\mathcal{W}^{(k)}$ we have

$$p=p^{(1)}+\left(p^{(2)}-p^{(1)}\right)+\cdots+\left(p^{(q)}-p^{(q-1)}\right)+\left(p-p^{(q)}\right) \tag{23}$$

Which is orthogonal decomposition of p and $p^{(k+1)}-p^{(k)}$ is the solution of the governing equation in $\mathcal{W}^{(k+1)}$. The illustrated $\chi_i^{(k)}$ and decomposition of the space are shown in Fig. 5 and Fig. 6.

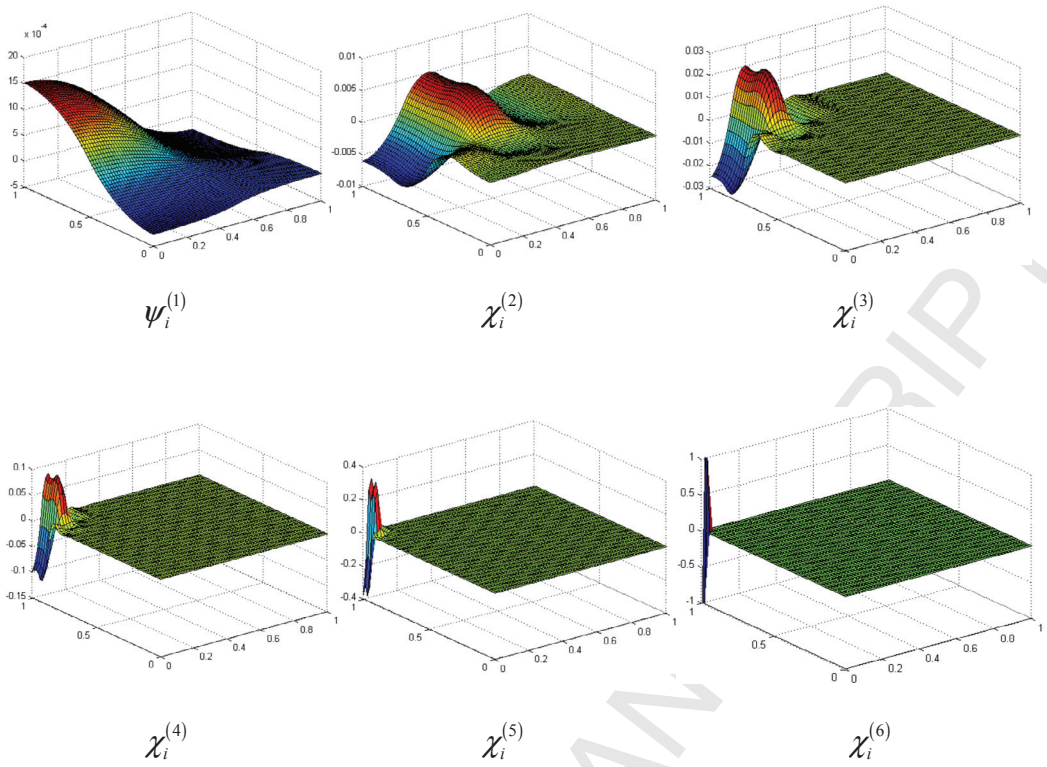

$\psi_i^{(1)}$ $\chi_i^{(2)}$ $\chi_i^{(3)}$

$\chi_i^{(4)}$ $\chi_i^{(5)}$ $\chi_i^{(6)}$

Fig.5 Illustration of $\chi_i^{(k)}$

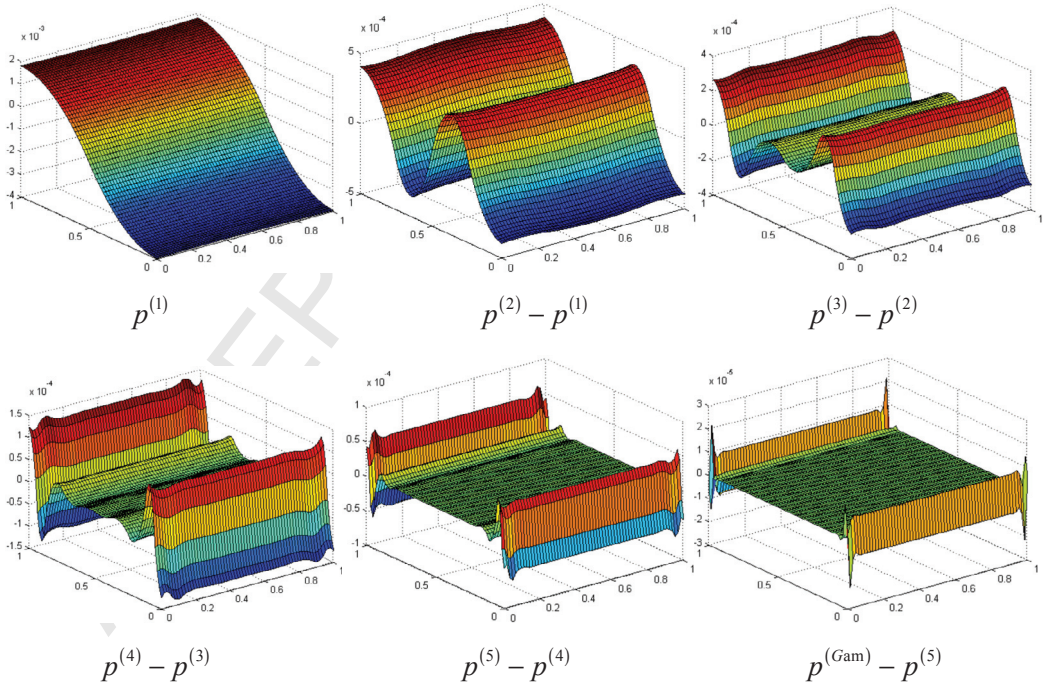

$p^{(1)}$ $p^{(2)}-p^{(1)}$ $p^{(3)}-p^{(2)}$

$p^{(4)}-p^{(3)}$ $p^{(5)}-p^{(4)}$ $p^{(Gam)}-p^{(5)}$

Fig.6 Illustration of decomposition of the space

For fractured porous media, we compute the pressure distribution of fractured porous media $p_f^{(k+1)}-p_f^{(k)}$ in each subspace $\mathit{\Pi}^{(k)}$, here $k\in\{1,...,q\}$. The influences

of fractures are captured in every level. The final pressure distribution of the whole media will be obtained by

$$p_f = p_f^{(1)} + \left(p_f^{(2)} - p_f^{(1)}\right) + \cdots + \left(p_f^{(q)} - p_f^{(q-1)}\right) + \left(p_f - p_f^{(q)}\right) \tag{24}$$

Algorithm **Multiresolution Decomposition Solve**

1: $A_{i,j}^{(q)} = A^f$ // Level q, $\mathcal{I}^{(q)} \times \mathcal{I}^{(q)}$ stiffness matrix

2: $\psi_i^{(q)} = \varphi_i$

3: $g_i^{(q)} = g_i$

4: **for** $k = q$ to 2 **do**

5: $B^{(k)} = W^{(k)} A^{f(k)} W^{(k),T}$

6: For $i \in \mathcal{J}^{(k)}$, $\chi_i^{(k)} = \sum_{i \in \mathcal{I}^{(k)}} W_{i,j}^{(k)} \psi_j^{(k)}$

7: $w^{(k)} = B^{(k),-1} W^{(k)} g^{(k)}$

8: $v^{(k)} = \sum_{i \in \mathcal{J}^{(k)}} w_i^{(k)} \chi_i^{(k)}$

9: $D^{(k,k-1)} = -B^{(k),-1} W^{(k)} A^{(k)} \bar{\pi}^{(k,k-1)}$

10: $R^{(k-1,k)} = \bar{\pi}^{(k-1,k)} + D^{(k-1,k)} W^{(k)}$

11: $g^{(k-1)} = R^{(k-1,k)} g^{(k)}$

12: $A^{(k\text{-}1)} = R^{(k-1,k)} A^{(k)} R^{(k,k-1)}$

13: For $i \in \mathcal{I}^{(k-1)}$, $\psi_i^{(k\text{-}1)} = \sum_{i \in \mathcal{I}^{(k)}} R_{i,j}^{(k\text{-}1,\mathrm{k})} \psi_j^{(k)}$

14: **end for**

15: $w^{(1)} = A^{(1),-1} g^{(1)}$

16: $p^{(1)} = \sum_{i \in \mathcal{I}^{(1)}} w_i^{(1)} \psi_i^{(1)}$

17: $p = p^{(1)} + v^{(2)} + \cdots + v^{(q)}$

The algorithm computes the stiffness matrix firstly according to section 2. Then the level q gamblets $\psi_i^{(q)}$ and the $g_i^{(q)}$ are introduced. The key step of this algorithm is the nested computation from line 4-line 14. The $A^{(k)}, g^{(k)}, \psi_i^{(k)}$ are regarded as inputs and $A^{(k\text{-}1)}, g^{(k\text{-}1)}, \psi_i^{(k\text{-}1)}$ are regarded as outputs. $w^{(1)}$ is computed outside the nested computation in line 15. The last step of the algorithm is to final solution p via addition of the subscale solution.

4. Numerical experiments

In the numerical examples provided here, the simulations of fluid flow in porous media are conducted using the multiresolution decomposition method described in above sections. Firstly, the multigrid method is validated for flow simulation in heterogeneous porous media. Then we extend this method to simulation of fluid flow in long-fractured media. We also consider the co-existence of small-scale fractures and long-scale fracture in this part. The efficiency of the multigrid method fracture network is investigated in the final numerical case. In this section, the discrepancies in pressure are measured using a relative L^2 norm

$$p_v = \frac{\left\| p_{\mathrm{f}} - p_{mg} \right\|_2^2}{\left\| p_{\mathrm{f}} \right\|_2^2} \tag{25}$$

Here, the reference pressure is denoted by p_{f}. The pressure computed with Multiresolution Operator Decomposition Method is denoted by p_{mg}.

4.1 Multiresolution decomposition method for heterogeneous case

The first numerical experiment is set to validate the multiresolution decomposition for heterogeneous porous media. A 1m×1m porous model with large number of small-scale fractures is considered, as depicted in Fig. 7(a). This model can be treated as a heterogeneous porous media with equivalent permeability field, as depicted in Fig. 7(b). The fluid flows from upper boundary to bottom boundary. The viscosity of fluid is μ= 1mPa·s. The left and right boundaries are treated as no-flow boundaries. The solution is obtained with q=4 as shown in Fig. 8.

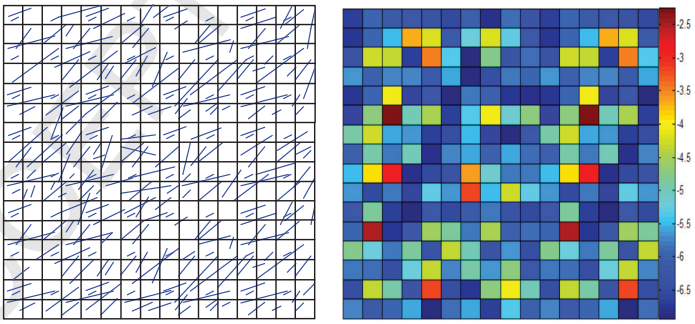

(a) **(b)**

Fig.7 Illustration of (a) physical model and (b) permeability field log(K), μm²

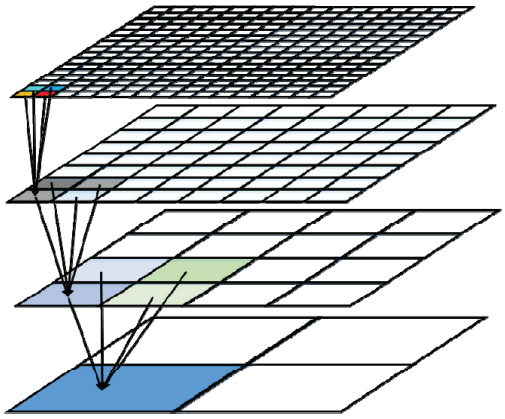

Fig.8 schematic of gamblets levels

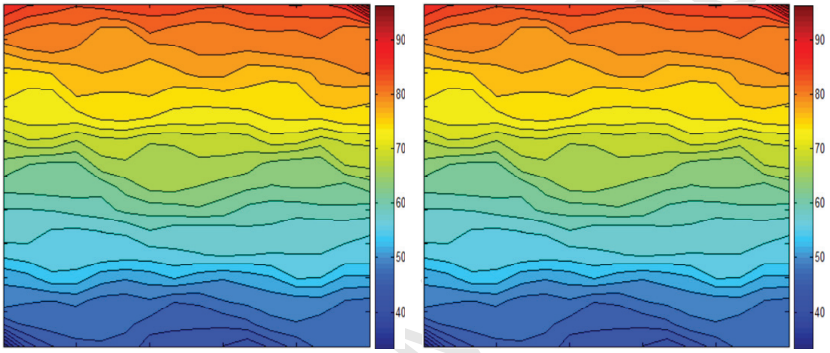

(a) **(b)**

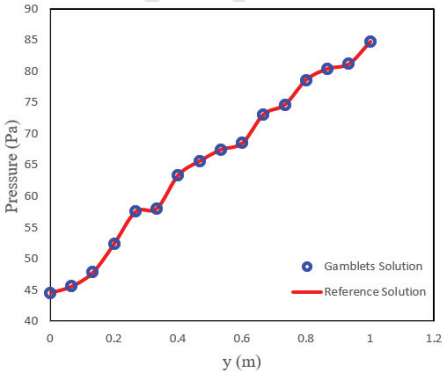

(c)

Fig.9 Comparison of FEM solution (a) and multiresolution decomposition solution (b)

The final numerical result of multigrid method is obtained by adding $p^{(k)} - p^{(k-1)}$ up. The Fig. 9 firstly shows the FEM solution and then compares the pressure distribution along x=0.5m with multiresolution decomposition solution. The figures show that this method could reflect the heterogeneity of the pressure distribution. The multiresolution decomposition method could track the reference solution very closely in the heterogeneous case. The pressure error measured with (25)

is 6.3×10^{-15}. It demonstrates that this method could effectively model fluid flow in porous media with heterogenous permeability field.

4.2 Multiresolution decomposition method for fractured porous media

The second numerical experiment is set to test the ability of this method to capture the influence of fracture. A 2D homogeneous porous medium (1m×1m) is considered , as shown in Fig. 10(a). The aperture of the fracture is a=1mm and the permeability is $K_f = a^2/12 = 8.33\times10^7$ mD. The fluid flows from upper boundary to bottom boundary. The viscosity of fluid is μ= 1mPa·s. Both left boundary and right boundary are set as no-flow boundaries. The DFM is solved on each subspace, and then the pressure distribution in fractured porous media is obtained by

$$p = p^{(1)} + \left(p^{(2)} - p^{(1)}\right) + \left(p^{(3)} - p^{(2)}\right) + \left(p - p^{(3)}\right)$$

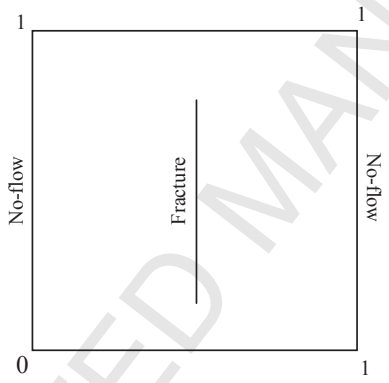

(a)

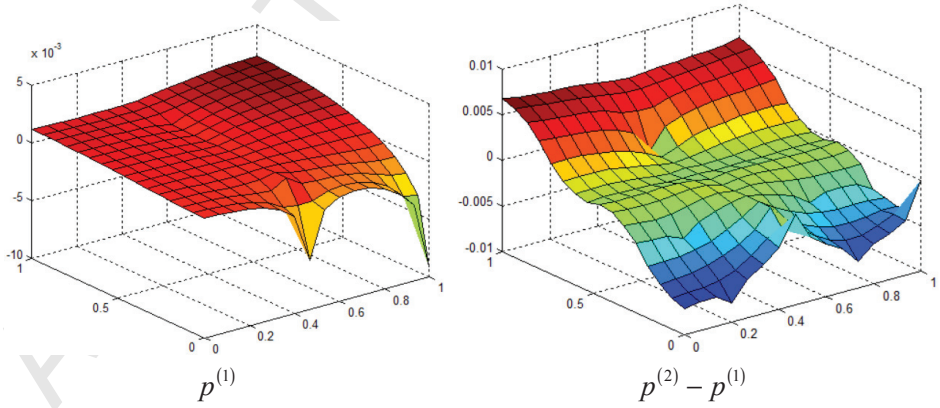

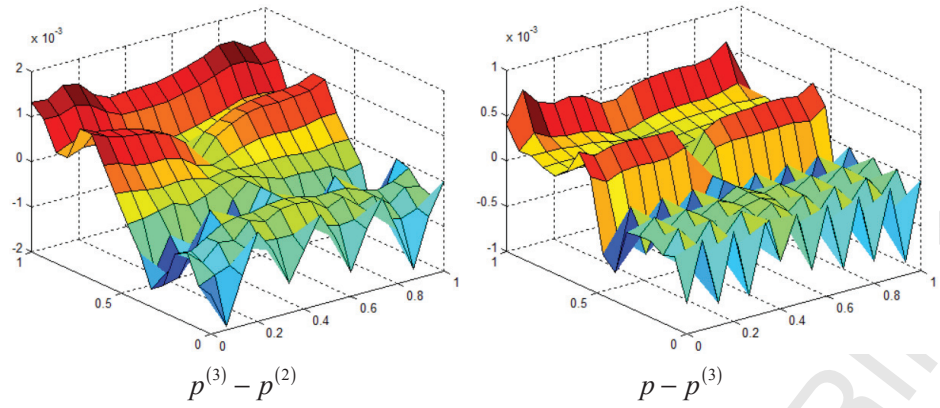

(b)

Fig.10 Model of fractured porous media (a) and multiresolution decomposition solution (b)

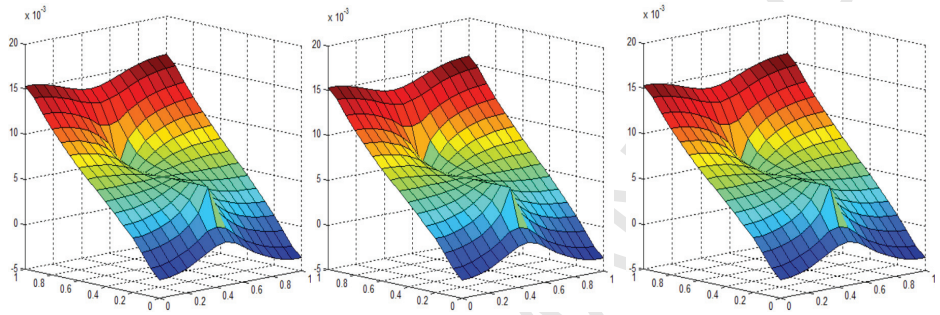

(a) **(b)** **(c)**

Fig.11 Comparison of FEM solution (a) and gamblets solution *q*=4(b) and *q*=2(c)

Results for pressure distributions $p^{(k)} - p^{(k-1)}$ are shown in Fig. 10(b). It is obvious that the multigrid method could capture the influence of fracture on every level. Then we sum $p^{(k)} - p^{(k-1)}$ up and obtain the final solution, as shown in Fig. 11. Comparison of pressure between FEM result and multiresolution decomposition results is shown in Fig. 12. The pressure error measured with relative L^2 norm is 4.2×10^{-5}. It demonstrates that the multigrid could model the divert effect of fracture effectively.

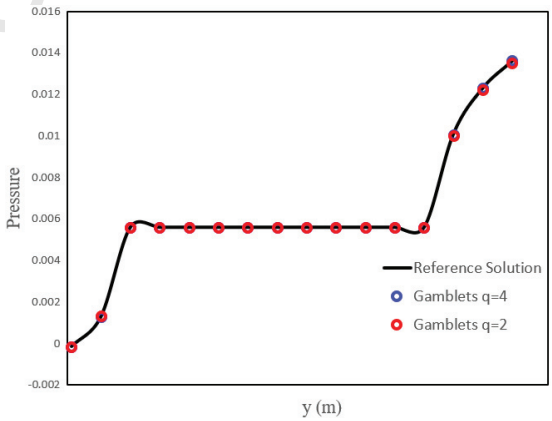

Fig.12 Comparison of FEM solution and multiresolution decomposition solution with q=4 and q=2

The decomposition of space may call multiscale methods up. Different from multiscale methods [17-18] that construct basis functions within coarse blocks, the basis functions of multiresolution decomposition method would not cause localized impact on the solution of fractured porous media, see Fig. 13(c). Here the physical model introduced above is studied with an injection well located at the bottom left corner and the production well located at the upper right corner. For the MsMFEM 5×5 coarse grid is used as shown in Fig. 13(a), the multiresolution decomposition solution is obtained with q=2. As shown in Fig. 13(b), the multiscale method could capture the influence of fracture effectively, but there are few errors near by the intersections of fracture and coarse block boundaries. This is caused by the coarse block boundary conditions used to compute multiscale basis functions [12]. In this experiment, no actions (e.g. oversampling technique, iterative procedure, global information and revised coarse boundary condition et al) are applied to improve the accuracy of the multiscale results.

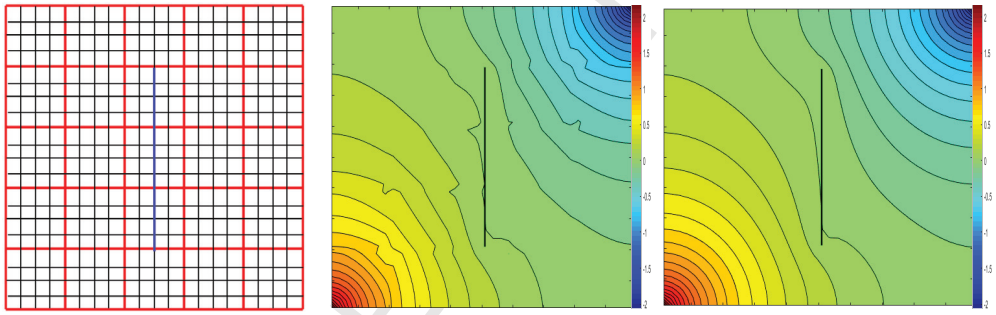

(a) **(b)** **(c)**

Fig.13 Multiscale Grid system (a) , multiscale solution(b) and multiresolution decomposition solution with q=2 (c)

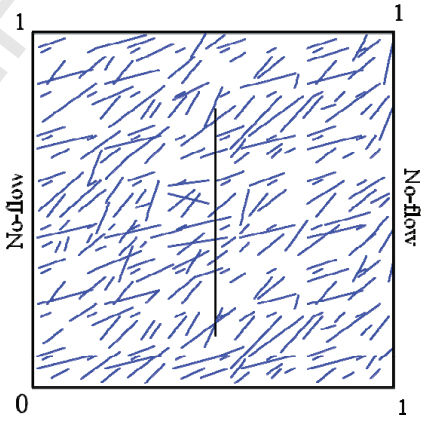

(a)

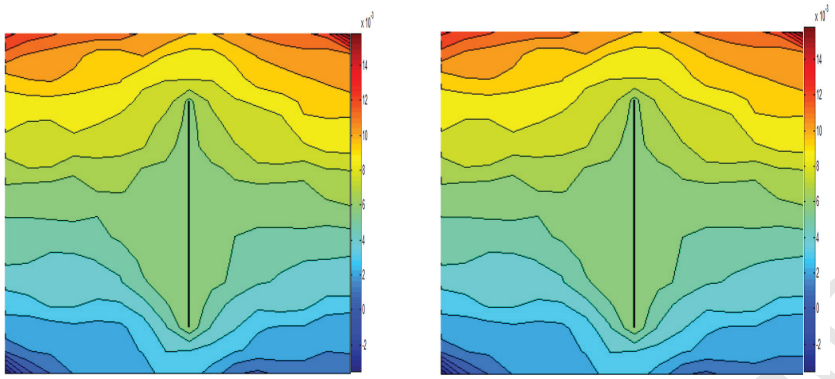

(b) (c)

Fig.14 Comparison of FEM solution (b) and multiresolution decomposition solution(c)

Then we take a further step and embed the long fracture into the heterogeneous porous media, see Fig. 14(a). From Fig. 14(b) we can observe the multigrid result is in close agreement with the fine-scale reference result. The pressure error measured using relative L^2 norm is 8.6×10^{-5}. It confirms that the presented multiresolution decomposition method is very robust for heterogenous permeability field in fractured porous media.

4.3 Multiresolution decomposition method for fracture network

The final experiment was presented to assess the accuracy of our multiresolution decomposition method for fracture network. Fracture network contains several intersected fractures and it will affect the pressure distribution significantly. An injection/production model with length scale 1m×1m is considered. Five fractures are contained in the porous media, as shown in Fig. 15. The injection well located at the bottom left corner and the production well located at the upper right corner. All boundaries are supposed to be no-flow boundaries. The apertures of the five fractures are a=1mm and the permeability are $K_f = a^2/12 = 8.33\times10^7$ mD.

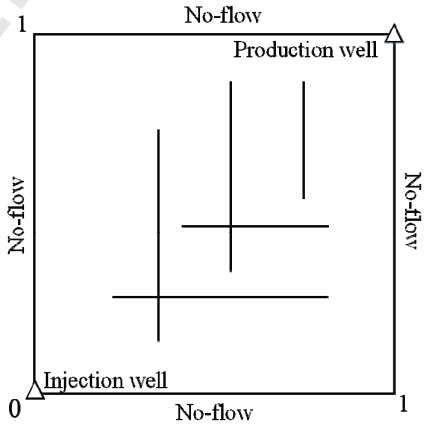

Fig.15 physical model of fractured network

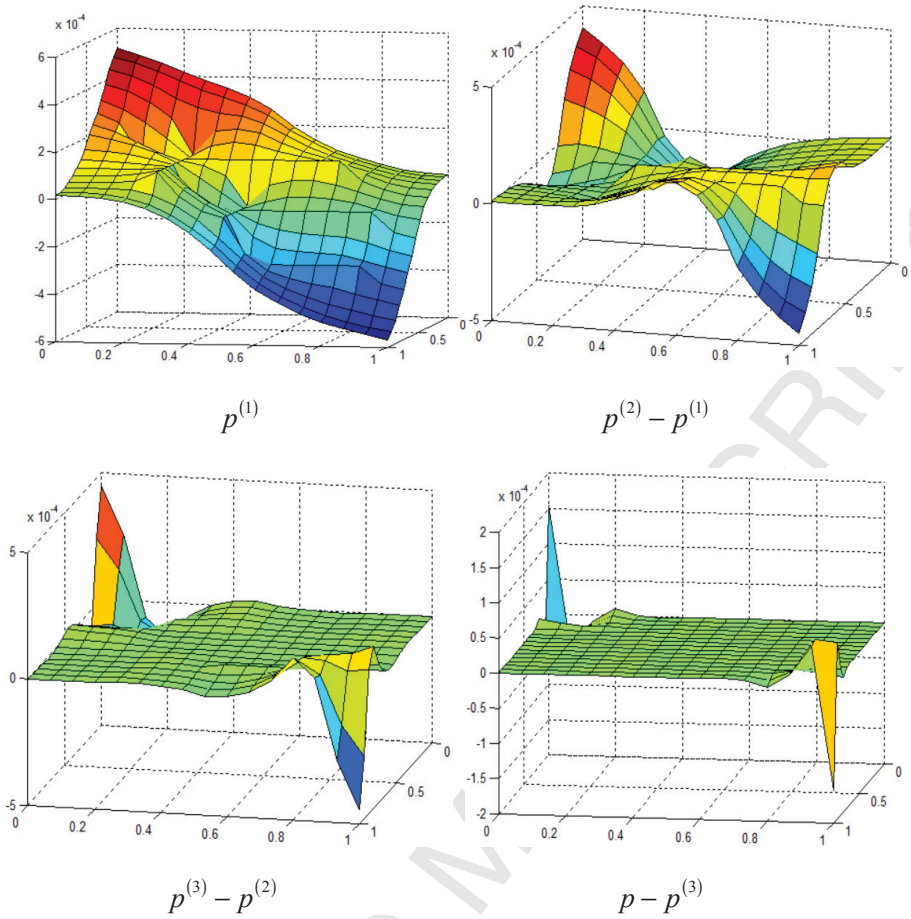

Fig.16 physical model of fractured network

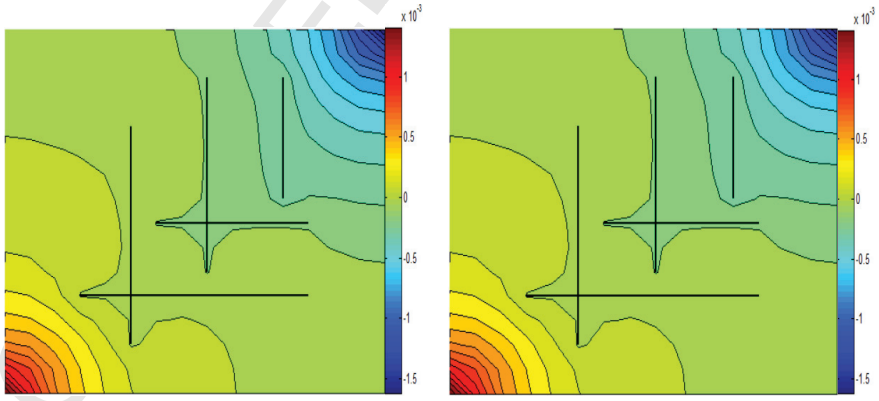

(a) **(b)**

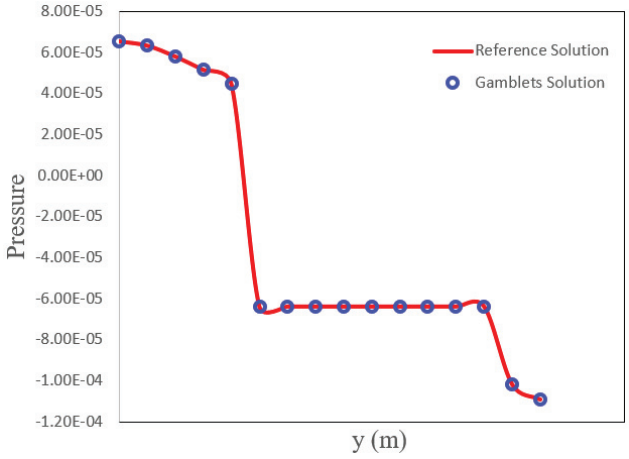

(c)

Fig.17 Comparison of FEM solution (a) and multiresolution decomposition solution(b)

In Fig. 16, we show the $p^{(k)} - p^{(k-1)}$ in different subspaces and the comparison of FEM solution and multiresolution decomposition solution is presented in Fig. 17. The pressure distribution shows that the proposed method effectively reflects the pressure distribution of fracture network. The pressure error measured using relative L^2 norm is 1.35×10^{-7}. The comparison implies that this method is able to reflect the interactions between fractures.

Although a fine mesh has been used to facilitate the presentation of the algorithm, this method is a meshless method. A fractured porous media with fracture network is investigated, as shown in Fig. 18(a). The fracture network consists of seven intersected fractures. We consider a triangular mesh as shown in Fig. 18(b) for simplicity. Let q=2 and the apertures of the seven fractures are a=1mm and the permeability are $K_f = a^2/12$ mD. The injection well located at the bottom left corner and the production well located at the upper right corner. All boundaries are supposed to be no-flow boundaries.

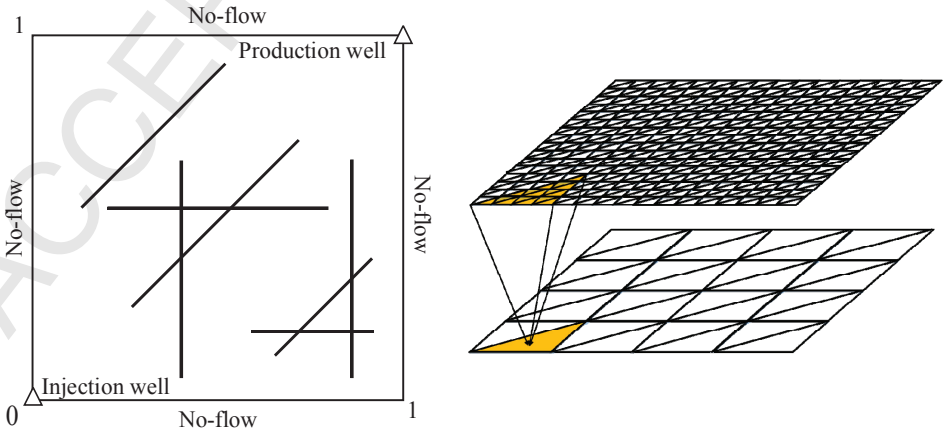

(a) **(b)**

Fig.18 Physical model of DFN (a) and gamblets levels (b)

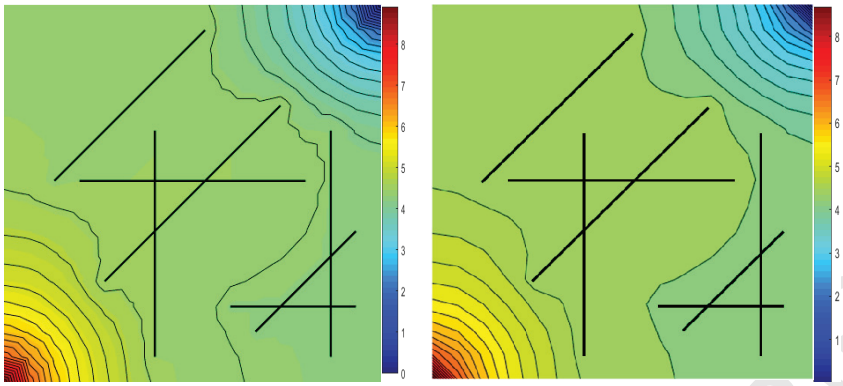

(a) (b)

Fig.19 FEM solution (a) and gamblets solution(b)

The pressure error measured using relative L^2 norm is 2.07×10^{-7}. We could see that this meshless method is effective for triangular mesh. For a given fractured porous domain, this method could run smoothly and effectively once the stiffness matrix, matrix W and matrix π are constructed. It is a robust method for simulation of complex fractured porous media.

5. Concluding remarks

In this work, we proposed an effective Multiresolution Operator Decomposition method for fluid flow in fractured porous media. This method could complete its fast simulation by decomposing the solution space into a direct sum of linear subspace that are orthogonal. Some numerical results presented in the paper demonstrate that the proposed formulation is an accurate and efficient method for flow simulation in fractured porous media. It may difficult to simulate fractured porous media with complicated fracture networks if the measurement functions are not adapted to the high conductivity fractures, especially when fractures are very close to each other, this is an ongoing work. The construction of gamblets can be completed independently with parallel computing method to further reduce computer memory and CPU time requirements. This work leads to the conclusion that the multigrid method is a significant development for the simulation of fluid flow in porous media.

Acknowledgements

The authors gratefully acknowledge support from National Science and Technology Major Project (2016ZX05060-010), the Fundamental Research Funds for the Central Universities (17CX06007), HO and FS gratefully acknowledges this work supported by the Air Force Office of Scientific Research and the DARPA EQUiPS

Program under award number FA9550-16-1-0054 (Computational Information Games) and the Air Force Office of Scientific Research under award number FA9550-18-1-0271 (Games for Computation and Learning).

References

1. Warren J.E., Root P.J. (1963). The behavior of naturally fractured reservoirs. Society of Petroleum Engineers Journal, 3(3): 245-255.
2. Kazemi H., Seth M.S., Thomas G.W. (1969). The interpretation of interference tests in naturally fractured reservoirs with uniform fracture distribution. Society of Petroleum Engineers Journal, 9(4): 463-472.
3. Lemonnier P., Bourbiaux B. (2010). Simulation of naturally fractured reservoirs. state of the art-part 1 matrix-fracture transfers and typical features of numerical studies. Oil Gas Science Technology, 65(2):263-286.
4. Ghorayeb K., Firoozabadi A. (2000). Numerical Study of Natural Convection and Diffusion in Fractured Porous Media. SPE Journal, 5(5): 12-20.
5. Huang Z.Q., Yao J., Wang Y.Y., Tao K. (2011). Numerical study on two-phase flow through fractured porous media. Science China Technological Sciences, 54(9): 2412-2420.
6. Karimi-Fard M., Firoozabadi A. (2001). Numerical Simulation of Water Injection in 2D Fractured Media Using Discrete Fracture Model. SPE Reservoir Evaluation & Engineering.
7. Hauge V.L., Aarnes J.E. (2009). Modeling of Two-Phase Flow in Fractured Porous Media on Unstructured Non-Uniformly Coarsened Grids. Transport in Porous Media, 77(3): 373-398.
8. Huang Z.Q., Yao J., Wang Y.Y. (2011). Numerical study on waterflooding development of fractured reservoir with discrete-fracture model. Chinese J Comput Phys, 28: 148-156.
9. Hoteit H., Firoozabadi A. (2008). An efficient numerical model for incompressible two-phase flow in fractured media. Advances in Water Resources, 31(6): 891–905.
10. Christie M.A. (1996). Upscaling for reservoir simulation. J. Pet. Tech., 48: 1004–1010.
11. Durlofsky L.J. (1991). Numerical calculations of equivalent gridblock permeability tensors for heterogeneous porous media. Water Resour. Res., 27: 699–708.

12. Hou T.Y., Wu X.H. (1997). A Multiscale Finite Element Method for Elliptic Problems in Composite Materials and Porous Media. Journal of Computational Physics, 134(1): 169-189.
13. Efendiev Y.R., Wu X.H. (2002). Multiscale finite element for problems with highly oscillatory coefficients[J]. Numerische Mathematik, 90(3): 459-486.
14. Aarnes J.E., Kippe V., Lie K.A. (2005). Mixed multiscale finite elements and streamline methods for reservoir simulation of large geomodels. Advances in Water Resources, 28(3): 257–271.
15. Jenny P., Lee S.H., Tchelepi H.A. (2003). Multi-scale finite-volume method for elliptic problems in subsurface flow simulation. Journal of Computational Physics, 187(1): 47–67.
16. Tene Matei., Al Kobaisi M.S., Hajibeygi H. (2016). Algebraic multiscale method for flow in heterogeneous porous media with embedded discrete fractures (F-AMS). Journal of Computational Physics, 321: 819-845.
17. Zhang Q., Huang Z., Yao J., Wang Y., Li Y. (2017). A multiscale mixed finite element method with oversampling for modeling flow in fractured reservoirs using discrete fracture model. Journal of Computational & Applied Mathematics, 323: 95-110.
18. Qingfu Zhang, Zhaoqin Huang, Jun Yao, Yueying Wang, Yang Li (2017). Multiscale mimetic method for two-phase flow in fractured media using embedded discrete fracture model. Advances in Water Resources, 107: 180-190.
19. Gulbransen A., Hauge V.L., Lie K.A. (2009). A multiscale mixed finite element method for vuggy and naturally fractured reservoirs. SPE Journal, 15(15): 395-403.
20. Brandt A. (1973). Multi-level adaptive technique (MLAT) for fast numerical solution to boundary value problems[M]. Proceedings of the Third International Conference on Numerical Methods in Fluid Mechanics. 82-89.
21. Hackbusch W. (1978). A fast iterative method for solving poisson's equation in a general region. Numerical Treatment of Differential Equations. Springer Berlin Heidelberg. 51-62.
22. Fedorenko R.P. (1961). A relaxation method of solution of elliptic difference equations, Mat. i Mat. Fiz. 922-927.
23. Yavneh I. (2006). Why multigrid methods are so efficient. Computing in Science Engineering. 8(6): 12-22.
24. Engquist B., Luo E. (1997). Convergence of a multigrid method for elliptic

equations with highly oscillatory coefficients. SIAM Journal on Numerical Analysis. 34(6): 2254-2273.

25. Wan W. L., Smith T.F.C.B. (2000). An energy-minimizing interpolation for robust multigrid methods. SIAM J.sci.comput. 21(4): 1632-1649.
26. Ruge J.W., Stüben K. (1987). Algebraic multigrid. Multigrid Methods S.f.mccormick Frontiers in Applied Mathematics: 73-130.
27. Yserentant H. (1986). On the multilevel splitting of finite element spaces. Numer Math, 49(4): 379-412.
28. Bank R.E., Dupont T.F., Yserentant H. (1988). The hierarchical basis multigrid method. Numerische Mathematik, 52(4): 427-458.
29. Vassilevski P. (1989). Multilevel Preconditioning Matrices and Multigrid V-Cycle Methods. Robust Multi-Grid Methods. 23: 200-208.
30. Branets L.V., Ghai S.S., Lyons S.L., Wu X.H. (2009). Challenges and technologies in reservoir modeling. Communications in Computational Physics, 6(1): 1-23.
31. Owhadi H. (2015). Multigrid with rough coefficients and multiresolution operator decomposition from hierarchical information games. Computer Science.
32. Owhadi H., Scovel C. (2017). Universal scalable robust solvers from computational information games and fast eigenspace adapted multiresolution analysis. arXiv:1703.10761, 201.
33. Beylkin G., Coult N. (1998). A multiresolution strategy for reduction of elliptic pdes and eigenvalue problems. Applied & Computational Harmonic Analysis, 5(2): 129-155.
34. Brewster M.E., Beylkin G. (1997). A multiresolution strategy for numerical homogenization. Applied and Computational Harmonic Analysis, 2(4): 327–349.
35. Averbuch A., Beylkin G., Coifman R., Israeli M. (1998). Multiscale inversion of elliptic operators. Wavelet Analysis & Its Applications, 7(98): 341-359.
36. Zhang Y.T. (2005). Rock Hydraulics and Engineering (in Chinese). Beijing: China WaterPower Press
37. Yao J., Li Y.J., Huang Z.Q. (2009). Calculation of equivalent permeability tensors of fractured oil reservoirs using boundary element method (in Chinese). Pet Geol Recovery Eff, 16: 80–83.
38. Li Y.J., Yao J., Huang Z.Q. (2010). Calculation of equivalent permeability tensor and study on representative element volume for modelling fractured reservoirs (in Chinese). Chin J Hydrodyn Ser A, 25:1–7.

39. Wald A. (1945). Statistical decision functions which minimize the maximum risk. Annals of Mathematics, 46(2): 265-280.
40. Von Neumann J., Morgenstern O. (1944). Theory of Games and Economic Behavior. Princeton University Press, Princeton, NJ.
41. Nash J. (1951). Non-cooperative games. Annals of Mathematics, 54(2): 286-295.
42. Schäfer F., Sullivan T.J., Owhadi H. Compression, inversion, and approximate PCA of dense kernel matrices at near-linear computational complexity. arxiv.org/abs/1706.02205.
43. M Golomb., H Weinberger. (1959). Optimal approximation and error bounds. In On Numerical Approximation: Proceedings of a Symposium Conducted by the Mathematics Research Center, United States Army, at the University of Wisconsin, Madison, 117. University of Wisconsin Press.
44. Micchelli C.A., Rivlin T. J. (1977). A survey of optimal recovery. Ibm Research Symposia, 1-54.
45. H. Owhadi, L. Zhang, L. Berlyand. (2014). Polyharmonic homogenization, rough polyharmonic splines and sparse super-localization. ESAIM Math. Model. Numer. Anal., 48(2):517-552,.
46. Hughes T. J. R., Feijóo G. R., Mazzei L., Quincy J. B. (1998). The variational multiscale method—a paradigm for computational mechanics. Computer Methods in Applied Mechanics & Engineering, 166(1-2), 3-24.
47. Målqvist A., Peterseim D. (2014). Localization of elliptic multiscale problems. Mathematics of Computation, 83(290), 2583-2603.
48. Vassilevski P. S. (2010). General constrained energy minimization interpolation mappings for amg. , 32(1), 1-13.
49. Wan W. L., Chan T. F., Smith B. (2000). An Energy-minimizing Interpolation for Robust Multigrid Methods. Society for Industrial and Applied Mathematics. 21(4):1632-1649.
50. J Xu., Y Zhu. (2008). Uniform convergent multigrid methods for elliptic problems with strongly discontinuous coefficients. Mathematical Models & Methods in Applied Sciences, 18(01), 77-105.
51. Xu J., Zikatanov, L. (2004). On an energy minimizing basis for algebraic multigrid methods. Computing & Visualization in Science, 7(3-4), 121-127.
52. Brezina M., Mandel J., Vanek, P. (1999). Energy optimization of algebraic multigrid bases. Computing, 62(3), 205-228.
53. Chung E.T., Efendiev Y., Leung W. T. (2017). Fast online generalized multiscale

finite element method using constraint energy minimization. Journal of Computational Physics, 355.

54. Fu S., Chung, E.T. (2018). Constraint energy minimizing generalized multiscale finite element method for high-contrast linear elasticity problem.
55. J. Duchon. (1976). Interpolation des fonctions de deux variables suivant le principe de la flexion des plaques minces. Rev. Francaise Automat. Informat. Recherch Operationnelle Ser. RAIRO Analyse Numerique, 10(R-3):5-12,.
56. J. Duchon. (1978). Sur l'erreur d'interpolation des fonctions de plusieurs variables par les Dm-splines. RAIRO Anal. Numer., 12(4):325-334.
57. J. Duchon. (1978). Sur l'erreur d'interpolation des fonctions de plusieurs variables par les D^m-splines. RAIRO Anal. Numer., 12(4):325-334.
58. Harder R.L., Desmarais R.N. (1972). Interpolation using surface splines. Journal of Aircraft, 9(2), 189-191.
59. O'Hagan A. (1991). Bayes–hermite quadrature. Journal of Statistical Planning & Inference, 29(3), 245-260.
60. Shaw J. E. H. (1988). A quasirandom approach to integration in bayesian statistics. Annals of Statistics, 16(2), 895-914.
61. H. Wo´zniakowski. (2009). What is information-based complexity?, in Essays on the Complexity of Continuous Problems, Eur. Math. Soc., Zurich, 89-95.
62. H. Owhadi. (2015). Bayesian numerical homogenization, Multiscale Model. Simul., 13, 812-828